
This is an electronic reprint of the original article.
This reprint may differ from the original in pagination and typographic detail.

Kutinlahti, Veli-Pekka; Lehtovuori, Anu; Viikari, Ville

Amplifier-Antenna Array Optimization for EIRP by Phase Tuning

Published in:
2022 16th European Conference on Antennas and Propagation (EuCAP)

DOI:
[10.23919/EuCAP53622.2022.9768981](https://doi.org/10.23919/EuCAP53622.2022.9768981)

Published: 01/04/2022

Document Version
Peer-reviewed accepted author manuscript, also known as Final accepted manuscript or Post-print

Please cite the original version:
Kutinlahti, V.-P., Lehtovuori, A., & Viikari, V. (2022). Amplifier-Antenna Array Optimization for EIRP by Phase Tuning. In *2022 16th European Conference on Antennas and Propagation (EuCAP)* (pp. 1-5). Article 9768981 IEEE. <https://doi.org/10.23919/EuCAP53622.2022.9768981>

Amplifier-Antenna Array Optimization for EIRP by Phase Tuning

Veli-Pekka Kutinlahti, Anu Lehtovuori, and Ville Viikari

Abstract—In this paper, we analyse an antenna array fed with element-specific phase shifters and amplifiers. The elements of the array are mutually coupled and the operation of the amplifiers depend on the load impedance presented by the array. We derive a method for maximizing EIRP in a given direction and demonstrate the concept by simulations with 2x2 array fed with element-specific phase shifters and amplifiers at 2.5 GHz. Compared to the reference case, the optimization provides up to 0.7 dB improvement in EIRP in the -3 dB beam steering range.

I. INTRODUCTION

THE trend in transceiver systems is toward higher integration level. Many novel approaches have been proposed in the literature to obtain benefits and new functionality by re-designing amplifier-antenna interface. Both power amplifier (PA) and antenna are traditionally matched separately to a common reference impedance, often $50\ \Omega$, at the interface. Higher integration between the components can remove the need for separate matching circuits reducing component losses and complexity [1], [2]. However, the active input impedance of one element in an array depends on the feeding of the nearby elements, and load-pull characteristics of PA needs to be taken into account to maximizing efficiency, gain, or output power.

Utilizing the antenna structure as the power combining component for a Doherty power amplifier (DPA) is an exciting and inventive idea, which has gained interest in the last years. DPA is composed of two separate amplifiers, whose outputs are combined in arbitrary phase difference. The power combining, which is traditionally realized in a specific circuitry, can also be done on an antenna eliminating the need for combining circuitry and avoiding associated circuit losses [3], [4]. This method necessitates a multi-port antenna, where the coupling between the ports is properly adjusted for example using a coupling circuit.

PA-antenna integration with non- $50\text{-}\Omega$ interface and DPA-antenna system bring forth interesting approaches to helping to reduce circuit redundancies and complexity, as well as losses. Additional challenges arise however, when these individual

antennas are extended to antenna arrays. When active antennas are used to comprise antenna arrays or other systems of multiple antennas in close proximity, the behavior of the system is subject to non-linearity and distortion. Amplifier properties, such as its gain, efficiency and linearity, depend on the load impedance. On the other hand, the active input impedances of an antenna array depend on the input signals, which subsequently define also the beam direction and shape. Therefore, the whole antenna-amplifier array needs to be considered when selecting feeding phases in a beam steering array for example [5], [6].

As PA cannot be simultaneously matched to multiple impedances optimally, the dynamic impedance of beam steerable arrays is detrimental to the performance of the PA. Typical approach is to design arrays with minimal coupling to lower the effect of dynamic active impedance. Different techniques to lower coupling include decoupling networks [7]–[9], neutralization lines [10], high-impedance periodic structures [11], and electromagnetic band-gaps [12], [13]. Still, there might exist enough coupling in the antenna array to cause sufficient load pull to affect the PAs. Especially in arrays with large beam steering ranges, a PA should be tolerant of mismatching [14].

As mentioned, the PA non-linearity affects the input signals into the antenna elements, which in turn change the radiated fields. Studies this far have determined that active impedance affects mostly side-lobe levels [15], [16], but in large arrays there exists also a possibility of negative impedance at single element ports [17]. Calculating the behavior of amplifier or antenna array separately is simple as antenna by itself is linear, and input signals of amplifier can be chosen arbitrarily in modern active load-pull measurements. Modelling the combined behavior on the other hand is more complicated, because of multiple transmitters affecting each other. Multiple models for emulating the non-linear behavior of amplifiers in antenna arrays, or multi-port systems in general, have been devised [18], [19].

This paper presents a method for determining the phase shift values for highest EIRP in case where an antenna array is fed with load-dependent amplifiers. We demonstrate the method with an array, which has considerable coupling affecting the behavior, which affects the behavior of the amplifiers and thus radiated fields. To analyze the non-linear behavior of the system, we use a method similar to one described in [19], which has previously been used to predict the operation of coupled amplifiers. The result can be applied in designing and controlling practical beam-steerable antenna arrays and to the best of authors' knowledge, no such method has been presented previously.

Manuscript received Month NN, 2021; revised Month NN, 2021; accepted Month NN, 2021. Date of publication Month NN, 2021; date of current version Month NN, 2021. This work was supported by Business Finland, CoreHW, DA Design, Optenni, Radientum, SAAB Technologies, and Nokia Solutions and Networks through the RF Convergence Project. (*Corresponding author: Veli-Pekka Kutinlahti.*)

The authors are with the Department of Electronics and Nanoengineering, Aalto University School of Electrical Engineering, Espoo 02150, Finland (e-mail: veli-pekka.kutinlahti@aalto.fi; anu.lehtovuori@aalto.fi; ville.viikari@aalto.fi).

Digital Object Identifier 10.1109/LAWP2021.NNNNNNN

II. SYSTEM MODELING AND OPTIMIZATION

We focus on the general system described in Fig. 1. The system is composed of n -element antenna array with element specific phase shifter and amplifier feeding. The coupling of antennas causes an active impedance at the amplifier-antenna interface, which affects the behaviour of the amplifiers. This active impedance will dynamically vary when phases φ are varied to achieve beam steering. We assume ideal, continuously adjustable phase shifters and perfect matching between the phase shifters and amplifiers, that is b_{1i} waves are zero. In the following analysis, we derive a model which relates the phase shift values to radiated fields. We assume that we know how the output waves from the amplifiers depend on the input waves. We further model the antenna array with its S-parameters and radiation matrices. After we have derived the system model, we show how to use it for optimization.

A. Amplifier and Antenna Models

The input signal b_{2i} of an antenna element i is modelled with a complex function of the amplifier with two complex arguments as

$$b_{2i} = f_{2i}(a_{1i}, a_{2i}), \quad (1)$$

where a_{1i} is the input signal to the amplifier and a_{2i} is the reflected wave from the antenna. In other words, the output wave b_{2i} from an amplifier depends on the input signal a_{1i} as well as the load impedance, which is determined by b_{2i} and a_{2i} waves.

For convenience, the phases of the waves are normalized in respect to the phase φ_i of a_{1i} , which can be controlled freely because of ideal phase shifters. We can write (1) in form

$$b_{2i}e^{-j\varphi_i} = f_{2i}(|a_{1i}|, a_{2i}e^{-j\varphi_i}). \quad (2)$$

Finally, the exponent term is eliminated from the left side

$$b_{2i} = f_{2i}(|a_{1i}|, a_{2i}e^{-j\varphi_i})e^{j\varphi_i}. \quad (3)$$

Final form (3) has the convenience of transforming the reference of the phases from the global reference of the system to the local reference of the individual PAs and then back to the global reference. With an individual PA, changing of the phase φ_i has obviously no effect on the behavior.

The antenna array is modelled with S-parameters and element field patterns. S-parameters are used to calculate the active load impedance seen by the amplifiers under different excitations and element specific field patterns are used to relate excitations to generated far-fields. The two properties, active input impedance of the antenna array and the produced far-fields are connected to each other due to amplifiers' load-dependent operation. Element field pattern \mathbf{E}_{0i} relates the input voltage wave b_{2i} to the far field \mathbf{E}_i as

$$\mathbf{E}_i = \mathbf{E}_{0i}b_{2i}, \quad (4)$$

where the complex element field pattern vector contains field values at different angles as

$$\mathbf{E}_{0i} = [\mathbf{E}_{0i}(\theta_1, \phi_1), \dots, \mathbf{E}_{0i}(\theta_k, \phi_m)]^T, \quad (5)$$

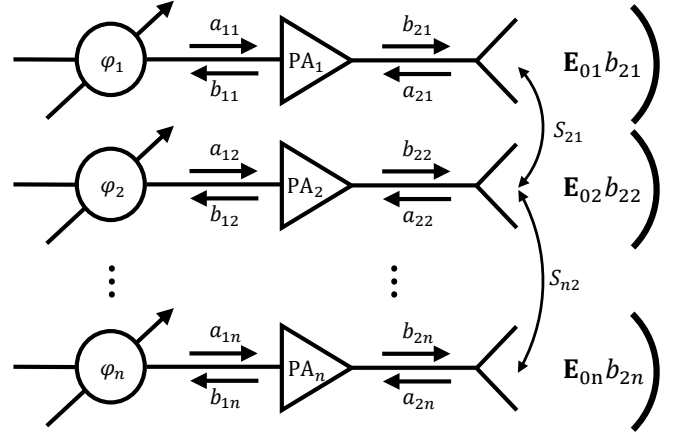


Fig. 1. System schematic.

The total field generated by the array is the sum of fields generated by elements

$$\mathbf{E}_{tot} = \sum \mathbf{E}_{0i}b_{2i}. \quad (6)$$

Waves travelling from antenna elements to amplifiers are calculated as

$$\mathbf{a}_2 = \mathbf{S}\mathbf{b}_2, \quad (7)$$

where $\mathbf{a}_2 = [a_{21}, \dots, a_{2n}]^T$ and $\mathbf{b}_2 = [b_{21}, \dots, b_{2n}]^T$.

B. System Model

The system model combines the individual models of the amplifiers and antenna array into a combined model, which takes into account the effect of the load impedance on PA's operation to find a stable solution for the waves \mathbf{a}_2 and \mathbf{b}_2 . Finally, with the converged solution, the total radiation pattern is calculated with (6).

In the system analysis, we aim to relate the input phase values φ in Fig. 1 to voltage waves \mathbf{b}_2 and \mathbf{a}_2 , which subsequently determine the radiated fields. To find the operation of the system with the selected phase shifts requires iteration. As \mathbf{a}_2 is dependent of \mathbf{b}_2 through antenna S-parameters, and \mathbf{b}_2 is then again dependent of \mathbf{a}_2 through amplifier operation described by (1), it naturally requires to solve the operation by consecutively solving \mathbf{b}_2 and \mathbf{a}_2 with each other. The convergent solution should be found.

To calculate the system behavior, waves \mathbf{a}_1 are kept constant for the calculation. The algorithm for our model is then as follows:

- 1) $b_{2i}^0 = f_{2i}(|a_{1i}|, 0)e^{j\varphi_i}$
- 2) $\mathbf{a}_2^{l+1} = \mathbf{S}\mathbf{b}_2^l$
- 3) $b_{2i}^{l+1} = f_{2i}(|a_{1i}|, a_{2i}^{l+1}e^{-j\varphi_i})e^{j\varphi_i}$
- 4) If $\max(|\mathbf{a}_2^{l+1}| - |\mathbf{a}_2^l|) < \delta$, terminate algorithm. Otherwise go to 2).

Our algorithm is simple to implement in MATLAB and agrees well with circuit level simulations in AWR.

C. Optimization

The presented system can be controlled by adjusting phase shifters, that is, phases of the waves fed to PAs. In an ideal system, only the phases of the antenna feeding weights would change with tuning of the phase shifters. In reality, also the amplitudes of the weights as well as the DC power consumption of the PAs will vary because of the PA load-pull effects when the active impedance of the antenna varies. This makes it possible to adapt the system operation through phase tuning. Phases can be chosen e.g., for the highest power-added efficiency, highest EIRP, etc.

In the following, we maximize the EIRP towards a given direction. Optimization is done with Nelder-Mead Simplex algorithm [20]. The objective function is EIRP towards a direction (θ, ϕ) , which for the system in Fig. 1 is

$$\text{EIRP}(\theta, \phi) = \frac{2\pi |\mathbf{E}_{\text{tot}}(\theta, \phi)|^2}{\eta} = \frac{2\pi |\sum \mathbf{E}_{0i}(\theta, \phi) b_{2i}|^2}{\eta}. \quad (8)$$

We assume identical power input to the PAs and only tune phases φ . The initial guess φ^0 is the progressively shifted phases, which maximize the EIRP of the amplifier-antenna system to the wanted direction (θ, ϕ) . The initial guess is found, by calculating the true operation of the system with the iterative algorithm described in section II.B. for all progressive phases and then selecting the one which maximizes the EIRP to the target direction (θ, ϕ) . Thus, it is not the same as in the ideal situation, when there is no coupling affecting the behavior of \mathbf{b}_2 -waves.

III. AMPLIFIER AND ANTENNA DESIGNS

To verify the proposed optimization method with simulations, we use a simple common collector BJT transistor amplifier. The design is presented in Fig. 2a. Fig. 2b shows the normalized $|b_2|$ of the amplifier with respect to the complex reflection coefficient $|a_2/b_2|$ from 0 to 0.95. The amplifier component values are listed in Table I and they are optimized

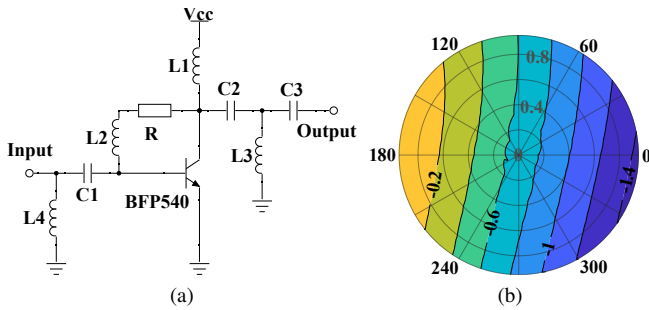


Fig. 2. (a) BJT amplifier schematic. (b) Normalized amplitude of amplifier output b_2 -wave in decibels with respect to the reflection coefficient of the load.

TABLE I
COMPONENT VALUES OF AMPLIFIER DESIGN.

Component	C1	C2	C3	R
Value	0.9 pF	2 pF	0.7 pF	5.6 k Ω
Component	L1	L2	L3	L4
Value	51 nH	51 nH	1.9 nH	5.1 nH

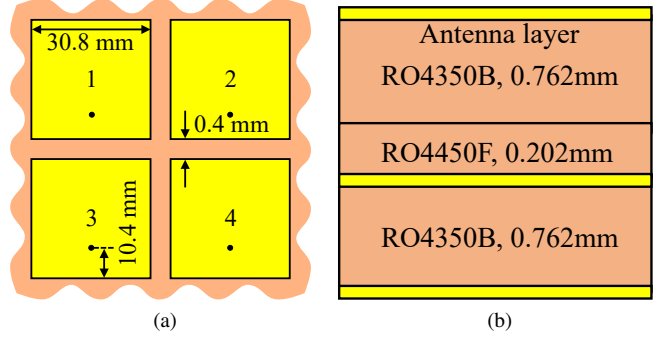


Fig. 3. (a) Array and antenna structure. Ground plane is a square with edge length of 123.2 mm. (c) Substrate structure.

with simulations in AWR to maximize power-to-load P_L at 2.5 GHz. The input and output are both matched to 50 Ω .

In contrast to a typical antenna array, where coupling is minimized, we have specifically designed the antenna with significant coupling by bringing elements very close to each other and have not used any coupling reducing techniques. This way, we imitate the effect of coupling in a larger array, where small element-to-element coupling, in the range of -15 dB, from multiple elements can produce high active reflection coefficient. Large arrays are difficult to measure because of practical reasons, and thus we have settled with a 4-element array.

The antenna array design used in this study is a simple 2x2 square patch antenna array. The elements are probe fed. The dimensions of the elements and the substrate structure are presented in Fig. 3. The S-parameters and radiation patterns

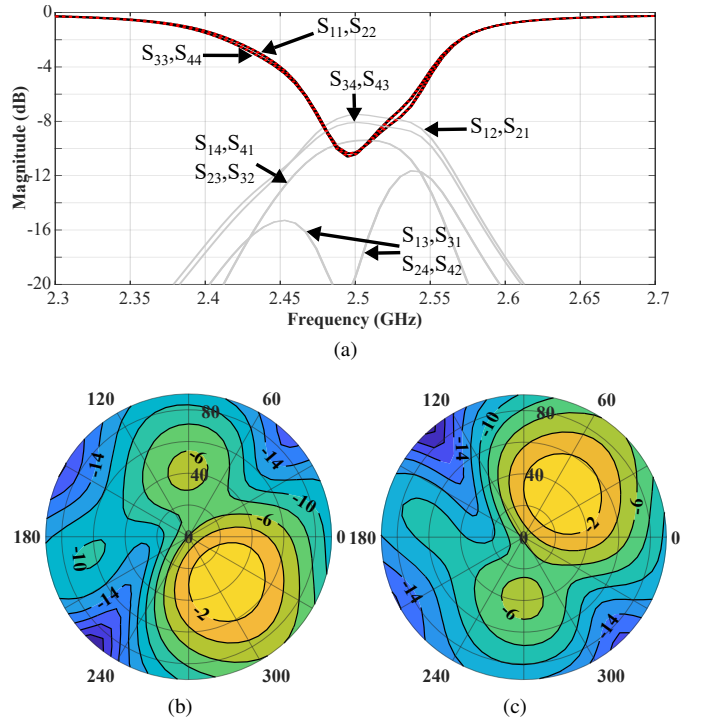


Fig. 4. (a) Antenna S-parameters. (b) and (c) Normalized EIRP patterns of the elements 1 and 3, respectively. Radius of the plot corresponds to θ -angle of the farfield and the angle of the plot corresponds to the ϕ -angle.

over the upper hemisphere $\theta = [0^\circ, 90^\circ]$ are shown in Fig. 4. Because of symmetry of the array, only patterns for elements 1 and 3 are presented as element patterns of 2 and 4 are similar but mirror with respect to E-plane.

IV. RESULTS

Fig. 5a shows the antenna EIRP envelope for the reference. The envelope has two local maxima, one at $(\theta, \phi) = (38^\circ, 90^\circ)$ and another at $(\theta, \phi) = (38^\circ, 270^\circ)$. Minimum θ of -3 dB beam steering range of EIRP is 45° at diagonals and maximum is 62° on the E-plane. Fig. 5b shows the improvement of the EIRP optimized with phase tuning compared to reference. Up to 0.7 dB improvement is achieved on the E-plane in the -3 dB beam steering range of the reference. On the diagonals there is no improvement, and in the $\theta < 40^\circ$ region there is no notable improvement.

To analyze further the reasons causing this improvement, we study the amplitude $|b_2|$ of elements 1 and 3 in Fig. 6. Both have a large areas with an improvement of over 0.1 dB and smaller areas with over 0.2 dB improvement. There exists some areas where $|b_2|$ is decreased with optimized phases. The phase tuning is taking into account the load-pull characteristic of the amplifiers and tries to make them work better in a situation with dynamic active impedance.

Around steer direction $(\theta, \phi) = (60^\circ, 90^\circ)$ both elements have their $|b_2|$ improved. This coincides with the area of with EIRP improvement of around 0.6 dB, that can be seen in Fig. 5b. As EIRP of the system in dB increases equally with increased b_2 power, as can be verified with (8), some of the improvement must come from other sources. The other source of improvement is from the better phasing of radiated fields.

Rather than considering the whole hemisphere, let's concentrate on the E-plane, where the greatest improvement is achieved at the -3 dB edge of the reference. Fig. 7 shows the behavior of active reflection coefficient (ARC) of element 1 with reference and optimized phases. The ARCs are superposed over the previously presented $|b_2|$ -plot of the amplifier model in Fig. 2b. It can be seen, that when beam steer angle is towards where EIRP is improved, it can be seen that the ARC of the optimized phases is moved towards the area where $|b_2|$ is maximized.

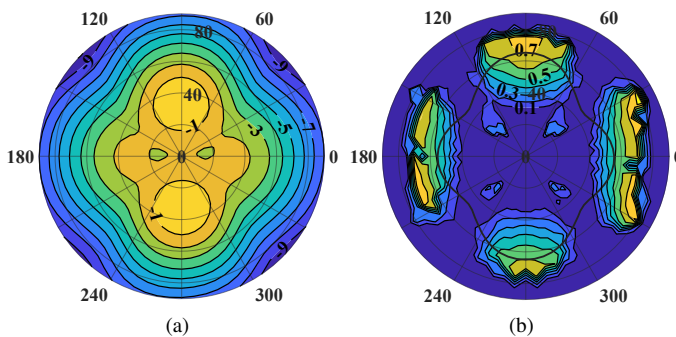


Fig. 5. (a) Beam steered normalized EIRP envelope of the reference case in dB. (b) Beam steered EIRP improvement envelope with optimization in dB and the -3 dB steer range of the reference. Radius of the plot corresponds to θ -angle of the farfield and the angle of the plot corresponds to the ϕ -angle.

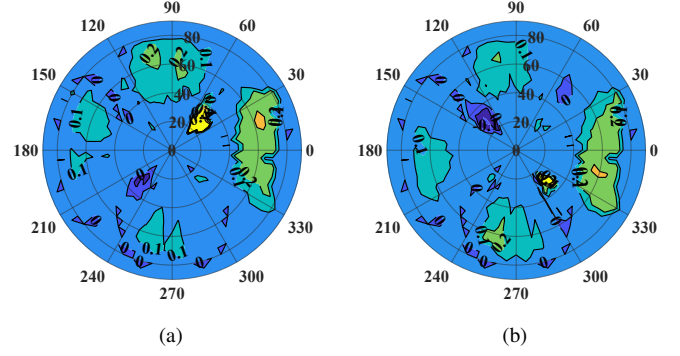


Fig. 6. $|b_2|$ of optimized feeds normalized to $|b_2|$ of reference for an element in dB. Radius of the plot corresponds to θ -angle of the farfield and the angle of the plot corresponds to the ϕ -angle. (a) Element 1. (b) Element 3.

V. CONCLUSION

We have optimized EIRP of an amplifier-antenna system with phase tuning. PAs connected to individual antenna element ports in a multiple-port antenna system exhibit load-pull because of interelemental coupling, which can be taken into account with knowledge of PA load-pull characteristics using an iterative simulation. We are able to improve EIRP of a 2×2 patch array with high coupling by up to 0.7 dB in the -3 dB beam steering range of the reference tuning method.

The improvement cannot be attained without taking the whole system behaviour into account, which includes the active impedance of the antenna and the load-pull of the amplifier. The concept of amplifier tuning with active impedance could also be used to maximize PAE or DC-consumption of the amplifiers, both of which would produce more energy efficient radiation systems.

REFERENCES

- [1] N. Hasegawa and N. Shinohara, "C-band active-antenna design for effective integration with a GaN amplifier," *IEEE Transactions on Microwave Theory and Techniques*, vol. 65, no. 12, pp. 4976–4983, 2017.
- [2] W. Liao, R. Maaskant, T. Emanuelsson, V. Vassilev, O. Iupikov, and M. Ivashina, "A directly matched PA-integrated K-band antenna for efficient mm-wave high-power generation," *IEEE Antennas and Wireless Propagation Letters*, vol. 18, no. 11, pp. 2389–2393, 2019.

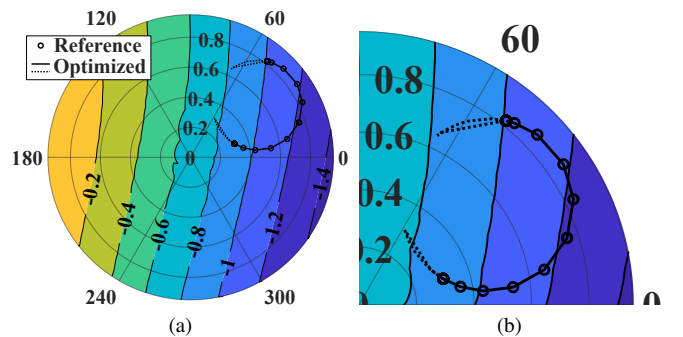


Fig. 7. Active reflection coefficient of element of 1 when beam is steered in the E-plane plotted over the complex plane. Fig. 2b is superposed on the background. Dashed line is for the areas where EIRP is improved with optimization. (a) General view, (b) upper right quarter.

- [3] O. A. Iupikov, W. Hallberg, R. Maaskant, C. Fager, R. Rehammar, K. Buisman, and M. V. Ivashina, "A dual-fed PIFA antenna element with nonsymmetric impedance matrix for high-efficiency doherty transmitters: Integrated design and ota-characterization," *IEEE Transactions on Antennas and Propagation*, vol. 68, no. 1, pp. 21–32, 2020.
- [4] H. Wang, S. Hu, T. Chi, F. Wang, S. Li, M. Huang, and J. S. Park, "Towards energy-efficient 5g mm-wave links: Exploiting broadband mm-wave doherty power amplifier and multi-feed antenna with direct on-antenna power combining," in *2017 IEEE Bipolar/BiCMOS Circuits and Technology Meeting (BCTM)*, 2017, pp. 30–37.
- [5] C. Fager, K. Hausmair, K. Buisman, K. Andersson, E. Sienkiewicz, and D. Gustafsson, "Analysis of nonlinear distortion in phased array transmitters," in *2017 Integrated Nonlinear Microwave and Millimetre-wave Circuits Workshop (INMMiC)*, 2017, pp. 1–4.
- [6] K. Hausmair, S. Gustafsson, C. Sánchez-Pérez, P. N. Landin, U. Gustavsson, T. Eriksson, and C. Fager, "Prediction of nonlinear distortion in wideband active antenna arrays," *IEEE Transactions on Microwave Theory and Techniques*, vol. 65, no. 11, pp. 4550–4563, 2017.
- [7] S. Chen, Y. Wang, and S. Chung, "A Decoupling Technique for Increasing the Port Isolation Between Two Strongly Coupled Antennas," *IEEE Transactions on Antennas and Propagation*, vol. 56, no. 12, pp. 3650–3658, 2008.
- [8] M. Li, L. Jiang, and K. L. Yeung, "Novel and Efficient Parasitic Decoupling Network for Closely Coupled Antennas," *IEEE Transactions on Antennas and Propagation*, vol. 67, no. 6, pp. 3574–3585, 2019.
- [9] —, "A Novel Wideband Decoupling Network for Two Antennas Based on the Wilkinson Power Divider," *IEEE Transactions on Antennas and Propagation*, vol. 68, no. 7, pp. 5082–5094, 2020.
- [10] S. Zhang and G. F. Pedersen, "Mutual Coupling Reduction for UWB MIMO Antennas With a Wideband Neutralization Line," *IEEE Antennas and Wireless Propagation Letters*, vol. 15, pp. 166–169, 2016.
- [11] G. Yang, J. Li, R. Xu, Y. Ma, and Y. Qi, "Improving the Performance of Wide-Angle Scanning Array Antenna With a High-Impedance Periodic Structure," *IEEE Antennas and Wireless Propagation Letters*, vol. 15, pp. 1819–1822, 2016.
- [12] W. E. McKinzie, D. M. Nair, B. A. Thrasher, M. A. Smith, E. D. Hughes, and J. M. Parisi, "60-GHz 2×2 LTCC Patch Antenna Array With an Integrated EBG Structure for Gain Enhancement," *IEEE Antennas and Wireless Propagation Letters*, vol. 15, pp. 1522–1525, 2016.
- [13] Bo Xu, K. Zhao, Z. Ying, S. He, and Jun Hu, "Investigation of surface waves suppression on 5G handset devices at 15 GHz," in *2016 10th European Conference on Antennas and Propagation (EuCAP)*, 2016, pp. 1–4.
- [14] B. Gashi, S. Krause, R. Quay, C. Fager, and O. Ambacher, "Investigations of active antenna doherty power amplifier modules under beam-steering mismatch," *IEEE Microwave and Wireless Components Letters*, vol. 28, no. 10, pp. 930–932, 2018.
- [15] S. R. Boroujeni, H. Al-Saedi, M. Nezhad-Ahmadi, and S. Safavi-Naeini, "Investigation of active load pulling effect on radiated power of the antenna elements in a finite phased array transmitter for satellite communication," in *2018 IEEE International Symposium on Antennas and Propagation USNC/URSI National Radio Science Meeting*, 2018, pp. 2159–2160.
- [16] M. Romier, A. Barka, H. Aubert, J. . Martinaud, and M. Soiron, "Load-pull effect on radiation characteristics of active antennas," *IEEE Antennas and Wireless Propagation Letters*, vol. 7, pp. 550–552, 2008.
- [17] H. Fan, Y. Ding, G. Goussetis, and M. J. Canavate Sanchez, "Antenna array driven by non-isolated power amplifiers for mimo applications," in *2019 49th European Microwave Conference (EuMC)*, 2019, pp. 468–471.
- [18] M. Romier, A. Barka, H. Aubert, J. P. Martinaud, and M. Soiron, "Iterative approach for the nonlinear simulation of active antennas," in *2009 IEEE Antennas and Propagation Society International Symposium*, 2009, pp. 1–4.
- [19] D. Nopchinda and K. Buisman, "Measurement technique to emulate signal coupling between power amplifiers," *IEEE Transactions on Microwave Theory and Techniques*, vol. 66, no. 4, pp. 2034–2046, 2018.
- [20] J. C. Lagarias, J. A. Reeds, M. H. Wright, and P. E. Wright, "Convergence properties of the nelder-mead simplex method in low dimensions," *SIAM Journal of Optimization*, vol. 9, no. 1, pp. 112–147, 1998.